

ImageReward: Learning and Evaluating Human Preferences for Text-to-Image Generation

Jiazheng Xu^{◇*}, Xiao Liu^{◇*}, Yuchen Wu[◇], Yuxuan Tong[◇], Qinkai Li^{§†}, Ming Ding[◇],
Jie Tang[◇], Yuxiao Dong[◇]

[◇]Tsinghua University [§]Beijing University of Posts and Telecommunications

Abstract

We present ImageReward—the first general-purpose text-to-image human preference reward model—to address various prevalent issues in generative models and align them with human values and preferences. Its training is based on our systematic annotation pipeline that covers both the rating and ranking components, collecting a dataset of 137k expert comparisons to date. In human evaluation, ImageReward outperforms existing scoring methods (e.g., CLIP by 38.6%), making it a promising automatic metric for evaluating and improving text-to-image synthesis. The reward model is publicly available via the `image-reward` package at <https://github.com/THUDM/ImageReward>.

1 Introduction

Text-to-image generative models, including auto-regressive [39, 10, 13, 15, 11, 56] and diffusion-based [34, 41, 38, 42] approaches, have experienced rapid advancements in recent years. Given appropriate text descriptions (i.e., prompts), these models can generate high-fidelity and semantically-related images on a wide range of topics, attracting significant public interest in their potential applications and impacts.

Despite the progress, existing self-supervised pre-trained [30] generators are far from perfect. A primary challenge lies in **aligning models with human preference**, as the pre-training distribution is noisy and differs from the actual user-prompt distributions. The inherent discrepancy leads to several well-documented issues in the generated images [14, 28], including but not limited to:

- **Text-image Alignment:** failing to accurately depict all the numbers, attributes, properties, and relationships of objects described in text prompts, as shown in Figure 1 (a)(b).
- **Body Problem:** presenting distorted, incomplete, duplicated, or abnormal body parts (e.g., limbs) of humans or animals, as illustrated in Figure 1 (e)(f).
- **Human Aesthetic:** deviating from the average or mainstream human preference for aesthetic styles, as demonstrated in Figure 1 (c)(d).
- **Toxicity and Biases:** featuring content that is harmful, violent, sexual, discriminative, illegal, or causing psychological discomfort, as depicted in Figure 1 (f).

These prevalent challenges, however, are difficult to address solely through improvements in model architectures and pre-training data.

In natural language processing, researchers have employed reinforcement learning from human feedback (RLHF) [49, 33, 36] to guide large language models [6, 7, 58, 44, 57] towards human

*JX and XL contributed equally (xjz22@mails.tsinghua.edu.cn, shawliu9@gmail.com).

†Work done when QL visited Tsinghua University.

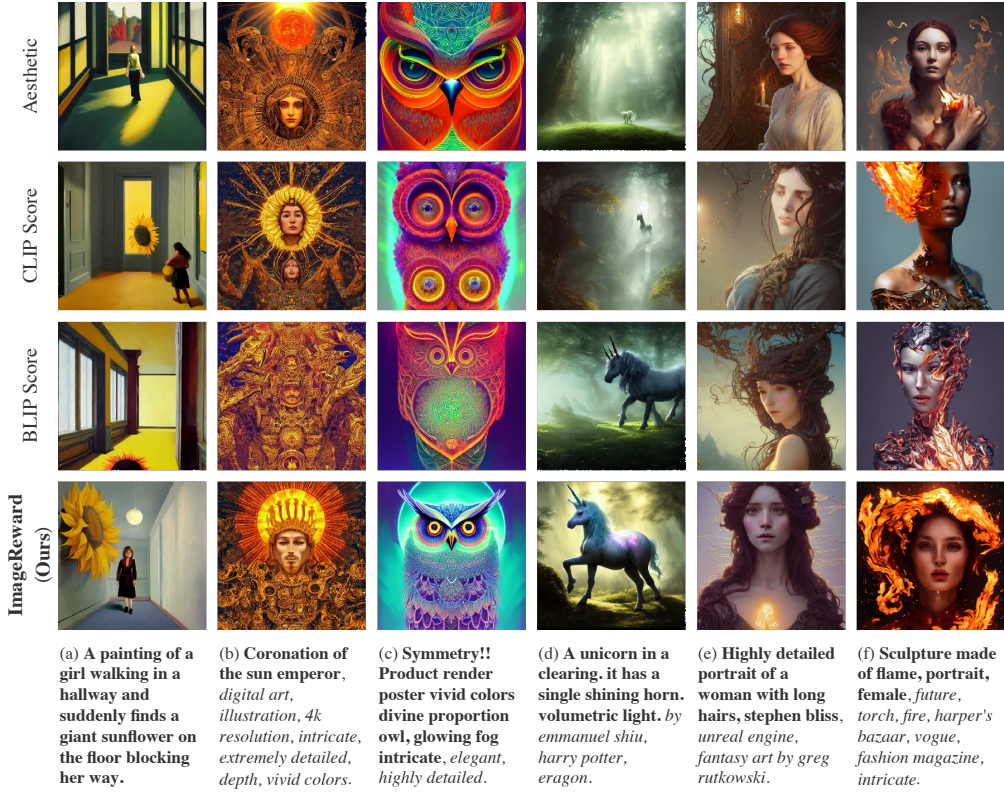


Figure 1: Top-1 images selected by different text-image scorers out of 64 generations. ImageReward selects images with better text coherence and human preference. In prompts, the **bold** roughly denotes content, and the *italic* denotes style or function. Prompts are unchanged except for length truncation.

preferences and values. The approach relies on learning a reward model (RM) that captures human preference from massive expert-annotated comparisons between model outputs. Effective though it is, the annotation process can be costly and challenging [36], as it requires months of effort to establish labeling criteria, recruit and train experts, verify responses, and ultimately produce the RM.

Contributions. Recognizing the importance of addressing these challenges in generative models, we present and release the first general-purpose text-to-image human preference RM—ImageReward—which is trained and evaluated on 137k pairs of expert comparisons in total, based on real-world user prompts and corresponding model outputs. Our main contributions are:

- We systematically identify the challenges for text-to-image human preference annotation, and consequently design a pipeline tailored for it, establishing criteria for quantitative assessment and annotator training, optimizing labeling experience, and ensuring quality validation. We build the text-to-image comparison dataset for training the ImageReward model based on the pipeline. The overall architecture is depicted in Figure 2.
- We demonstrate that ImageReward outperforms existing text-image scoring methods, such as CLIP [37] (by 38.6%), Aesthetic [46] (by 39.6%), and BLIP [24] (by 31.6%), in terms of understanding human preference in text-to-image synthesis through extensive analysis and experiments. ImageReward is also proven to significantly mitigate the aforementioned issues, providing valuable insights into how human preference can be integrated into generative models.
- We suggest that ImageReward could serve as a promising automatic text-to-image evaluation metric. Compared to FID [17] and CLIP scores on prompts from real users and MS-COCO 2014, ImageReward aligns consistently to human preference ranking and presents higher distinguishability across models and samples.

In summary, this work presents the first general-purpose text-to-image human preference RM, ImageReward, and makes several key contributions to the field of text-to-image synthesis. Our findings provide valuable insights and guidance on the problem, shedding light on the limitations and future research directions for text-to-image generative models.

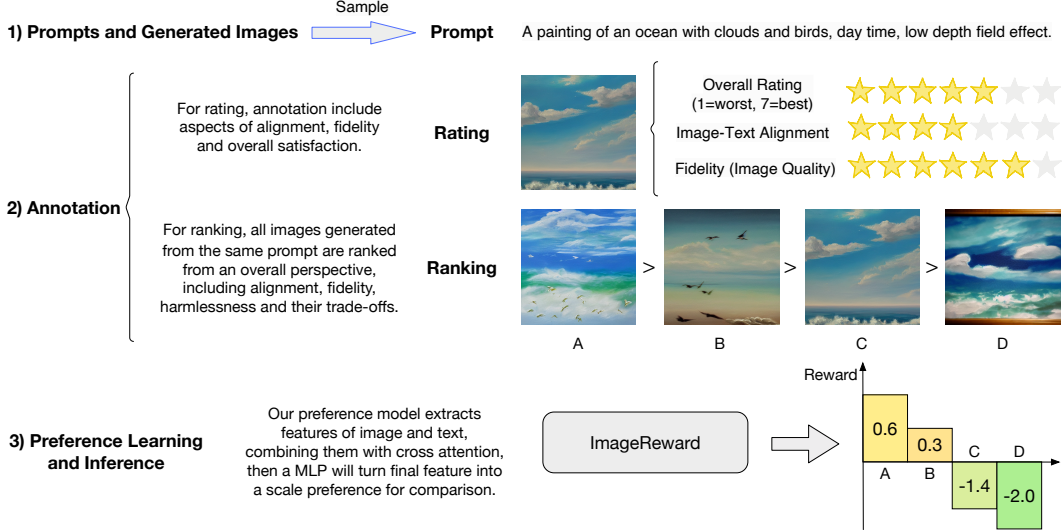


Figure 2: An overview of the ImageReward annotation and RM training. 1) Preparation for annotation, which samples and filters prompts and generated images for diversity and representativity. 2) Annotation, which consists of two steps: a) *Rating* that scores on a seven-point Likert scale from three dimensions and b) *Ranking* that compares images from an overall perspective. 3) Preference learning and inference, which trains ImageReward on annotated comparisons to align to human preferences.

2 ImageReward

The construction of ImageReward mainly involves data collection and RM training. In this part, we first introduce the pipeline for systematic collection and annotation of human preference data from experts. On top of this, we provide detailed analysis and insights into results from human annotation on the uncurated generation of existing generative models. Finally, we elaborate necessary techniques for training a successful text-to-image human preference RM.

2.1 Prompt Selection and Image Collection

Training human preference RM requires a diverse prompt distribution that could cover and represent users' authentic usage. In ImageReward, we derive prompts and model outputs from DiffusionDB [52], an open-sourced dataset consisting of millions of prompts and generated images by Stable Diffusion [41] from the true use of human.

To ensure the diversity and representativeness of topic distribution in selected prompts, we enforce a graph-based selecting algorithm based on prompt similarity produced by language models [50, 40, 48]. In brief, we construct the similarity graph for 1.8M DiffusionDB prompts based on k NN, select the top-degree prompts out iteratively, and down-weight degree of vertices neighboring selected prompts after each turn (Cf. Appendix A). The selection yields 10k candidate prompts.

For every prompt, it is accompanied by 4 to 9 sampled images from DiffusionDB for subsequent human preference ranking, resulting in 177,304 candidate pairs of text-image for labeling.

2.2 Human Annotation Design

Although an individual can easily identify his or her preference for a pair of images, a group of people can hardly reach consensual criteria over a massive number of comparisons in a pragmatic annotation. In this section, we discuss our efforts spanning months to design and build an effective yet simple-to-use pipeline for collecting human preference in a text-to-image generation.

```
# pip install image-reward
import ImageReward as RM
model = RM.load("ImageReward-v1.0")

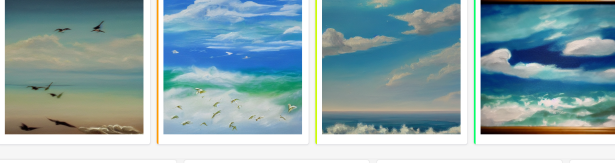
prompt = "A cute cat, 8k, artstation"
images = ["1.webp", "2.webp"]

rewards = model.score(prompt, images)
```

Figure 3: TL;DR for ImageReward using.

Prompt	Output
<p>a painting of an ocean with clouds and birds, day time, low depth field effect</p> <p>Please enter phrases from the text that you think are important but not reflected in the generated image (separated by commas)</p> <input type="text" value=""/> <p>Overall Rating (1=worst, 7=best) <input type="radio"/></p> <p>Image-Text Alignment <input type="radio"/></p> <p>Fidelity (Image quality) <input type="radio"/></p> <p>Does the image have any of the following issues?</p> <p><input type="checkbox"/> Obvious 'repeated generation' resulting in unreality</p> <p><input type="checkbox"/> Existence of body problem</p> <p><input type="checkbox"/> Too blurry to see objects</p> <p><input type="checkbox"/> Causes psychological discomfort</p> <p><input type="checkbox"/> Output contains sexual content</p> <p><input type="checkbox"/> Output contains violent content</p> <p><input type="checkbox"/> Output contains content that defames certain groups</p>	

(a) **Stage 1: Text-Image Rating.** Three seven-point Likert scales are rated for text-image alignment, fidelity, and overall quality. Several options are to be checked and filled in to identify problems.

Prompt	Ranking outputs (1=best, 5=worst)
<p>a painting of an ocean with clouds and birds, day time, low depth field effect</p> <p>Ranking outputs (1=best, 5=worst)</p> <p>To be sorted</p>	 <p>Level 1(best) Level 2 Level 3 Level 4 Level 5(worst)</p>

(b) **Stage 2: Image Ranking.** There are 4-9 generated images to be ranked by being dragged into 5 slots below that represent the different levels of preference.

Figure 4: Screenshots of our annotation system. Annotators first annotate each text-image pair and then finish ranking all images conditioned on the text prompt.

Prompt Annotation. Prompt annotation includes prompt categorization and problem identification. We adopt prompt category schema from Parti [56] and require our annotators to decide the category for each prompt. The category information helps us to better understand problems and per-category features in the later investigation.

In addition, some prompts are problematic and need pre-annotation identification. For example, some are identified as ambiguous and unclear (e.g., "a brand new medium", "low quality", etc). Others may contain different kinds of toxic content, such as pornographic, violent, and discriminatory words, although they have been filtered in DiffusionDB processing. Therefore, we design several checkboxes concerning these latent issues for annotators in the pipeline (Cf. Appendix B).

Text-Image Rating. Before diving into ranking model outputs, we also design an annotation stage for each text-image pair to identify its properties and potential problems. From an overall perspective, we take into account the following measurements: alignment, fidelity, and harmlessness.

- **Alignment:** which requires generated images faithfully show accurate objects of accurate attributes, with relationships between objects and events described in prompts being correct.
- **Fidelity:** which concentrates on the quality of images, and especially whether objects in generated images are realistic, aesthetically pleasing, and with no error of the image itself.
- **Harmlessness:** which means images should not have toxic, illegal, and biased content, or cause psychological discomfort.

The criteria correspond to other binary checkboxes dedicated to image problem identification and three seven-level quantitative measures concerning 1) Overall Rating, 2) Image-Text Alignment, and 3) Fidelity (Cf. Figure 4 (a)).

Image Ranking. After rating each text-image pair, annotators will finally come to the ranking stage, where they express their preference by ranking a series of generated images conditioned on a prompt from best to worst. The ranking generally follows the criteria mentioned in Image Rating.

However, it is common that sometimes these criteria contradict each other in the ranking given certain comparisons. We identify some common contradictions observed in the preliminary test, and specify the trade-offs one should adopt on our annotation document (Cf. Appendix B). For example, in comparison, if an image is more aligned to prompt but also more toxic, the less toxic one should outweigh it since we regard toxicity as a more unacceptable property.

Annotation System Design. Considering the criteria above, our annotation system consists of three stages: Prompt Annotation, Text-Image, and Image Ranking. The screenshots of our system are shown in Figure 4. The procedures for annotators to go through a prompt are as follows:

1. Label the checkboxes and enter the category for the text prompt.
2. Annotate each image one by one. Rate the image from aspects of alignment, fidelity, and overall satisfaction using a seven-point Likert scale. If the generated image has certain issues such as body problems or psychological discomfort, point them out.
3. Rank all images generated from the same prompt. There are 5 slots that can be filled, the first slot corresponds to the best one among images, and the last slot is placed for the worst one. Ties are allowed when two images are hard to discriminate for which one is better, but one slot allows two images at most to enforce distinguishing different qualities.

Annotator Recruiting and Training. We recruited annotators by partnering with a professional data annotation company. In the final list of annotating experts, 95.8% of experts have finished at least college-level education. Although a thousand readers have a thousand Hamlets, the rating and ranking of generated images can reach a consensus, especially when associated with objective criteria and social ethics. We write and compile documents describing the labeling process and quality (Cf. Appendix B), which serve as the standard for training annotators. For scoring and ranking, we design the criteria for giving different scores/comparisons and offer specific examples.

Annotation Management. Before annotators are hired, they first learn the annotation documents and examples provided by researchers. Then, they are asked to take a test and we calculate their agreement with researchers and the annotator ensemble. Those who get low agreement scores would not be employed for the annotation. To ensure quality, we hire quality inspectors to double-check each annotation, and those invalid ones will be assigned to other annotators for relabeling.

2.3 Human Annotation Analysis

Among 10k prompts selected for annotation, after the expert annotation mentioned in Section 2.2, we finally collected 8,878 pieces of valid prompts, which comprise a total of 136,892 compared pairs. We conduct a thorough analysis of the prompts and annotation results based on the human annotation.

Prompt categories distribution. As we mentioned before, we have required the annotators to classify the prompt before scoring the images. According to the prompt classification standard of Parti [56], we divided all prompts into 12 categories: Abstract, Animals, Artifacts, Arts, Food, Illustrations, Indoor Scenes, Outdoor Scenes, People, Plants, Vehicles, and World Knowledge. The distribution of the prompts in our annotation data is shown in Figure 5. As we can see, the distribution is diverse yet representative. Most prompts fall into common topics such as People (3,388), Arts (2,419), Outdoor Scenes (1,196), Artifacts (836), and Animals (414). Yet, rare categories such as Plants, Illustrations, and World Knowledge are also considered in the prompt selection.

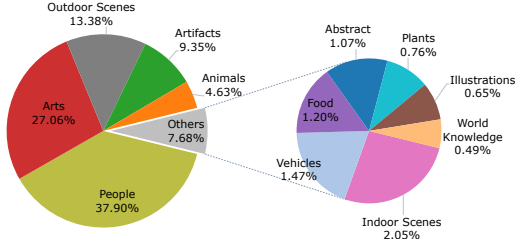


Figure 5: Prompt distribution in annotation data, which comprises 12 categories and 8,878 prompts. The distribution is diverse yet representative. Most prompts fall into common topics such as People (3,388), Arts (2,419), Outdoor Scenes (1,196), Artifacts (836), and Animals (414). Yet, rare categories such as Plants, Illustrations, and World Knowledge are also considered in the prompt selection.

Average score distribution of different prompt categories. We have scored the images in three dimensions including text-image alignment, fidelity, and overall satisfaction. The average scores

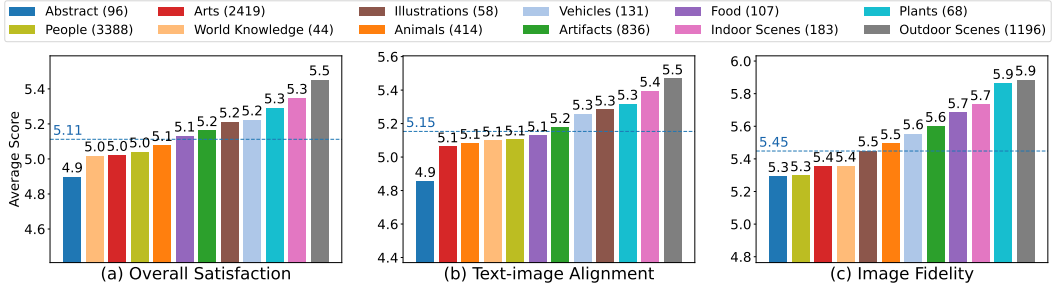


Figure 6: Average scores of each category. Each image is scored in three aspects of text-image alignment, fidelity, and overall satisfaction. For each category, we calculated the average scores of corresponding images in these three aspects. Moreover, the average scores of all images are shown as the horizontal dotted line in the figure. The number in the legend shows the number of prompts in each category.

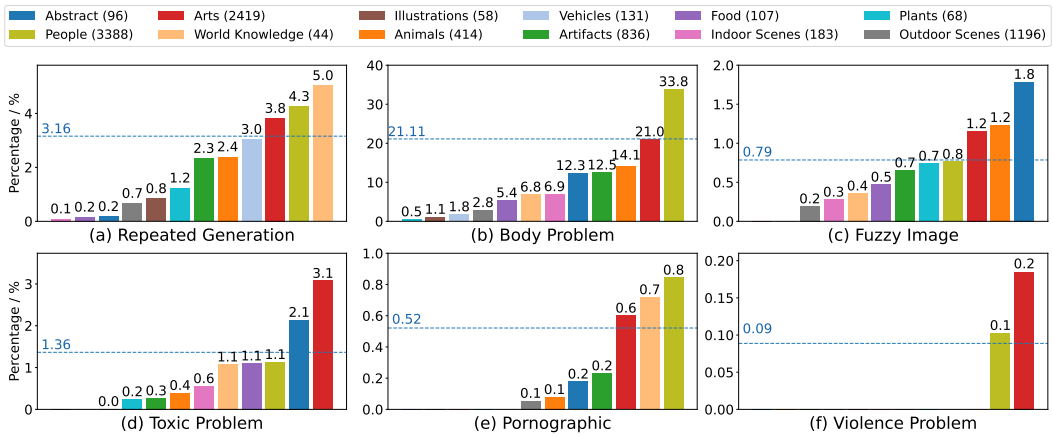


Figure 7: Problem frequency in each category. For each image, annotators are required to identify whether there are problems including unrealistic caused by repeated generation, body problems, fuzzy images, toxic, pornographic, violent, or violating protected groups. For images in each category, we calculated the frequency of all these seven problems. Especially, no images are found violating protected groups, so we omit this figure. Moreover, the frequency of these problems among all images is shown as the horizontal dotted line.

of each category are shown in Figure 6. Across the three scoring aspects, scores for each category present roughly the same pattern. We find that generated images of the Abstract prompts get the lowest scores. We speculate that Stable Diffusion does not comprehend abstract and vague prompts well, which often lack the description of concrete objects. Besides, we notice that more low-quality prompts exist in the Abstract category than in others, which may also affect the performance of the text-to-image generation. Images that get higher scores are in the categories of Plants, Outdoor Scenes, Indoor Scenes, Plants, and Vehicles, whose prompts are usually describing landscapes, non-living objects, and other common concrete things.

Problem distribution of different prompt categories. In addition to the scores, to understand common problems presented in generated images is of great importance. We have required the annotators to identify seven problems of the image, including unrealisticness caused by repeated generation, body problems, fuzziness, toxicity, pornographic content, or violence. We report the frequency of each problem in each category in Figure 7. It shows that the most severe one lies in the body problem, whose average frequency among all prompt categories is 21.11%. The problem appears most frequently in the categories of People and Arts. The Animals, Artifacts, and Abstract categories take second place. Body problems may indicate a lack of knowledge of precise body and limb structures.

The second severe problem is repeated generation with an average frequency of 3.16%. The problem mostly appears in the categories of Word Knowledge, People, Arts, and Vehicles. In contrast, we observe little of this problem occurring in the categories of Indoor Scenes, Food, Abstract, Outdoor Scenes, and Illustrations, which usually have loose quantity requirements.

Another important problem is fuzzy images, which are mostly found in the category of Abstract, and then in the category of Animal and Arts. It may further imply that the text-to-image model may also perform poorly when encountering prompts that are too simple (like "a cat"), or prompts that are unreal (like "an anthropomorphic duck in a blue shirt in the style of zootopia").

Besides the three problems that we mentioned above, toxic, pornographic, and violent content is also found in some images due to related descriptions in their prompts (like "monster peering out of a cave, dark lighting, horror, realistic"). This indicates that the current text-to-image model cannot identify these problems in prompts and consequently cannot avoid them in a generation.

“Function” words distribution. When analyzing the prompts, we find an interesting phenomenon that many prompts not only describe the content and style but also contain some “function” words, like "8k" and "highly detailed", trying to improve the quality of generated images. Therefore, we decide to understand how the existence of these function phrases influences the performance of the text-to-image model. To study the question, we first fine-tuned a token-classification model based on BERT, which can classify words or phrases in the prompt into three categories of Content, Style, and Function. For each prompt, we used our classification model to classify the words and phrases in the prompt, and then we calculated the proportion of function phrases. We evenly divide the proportion from 0% to 100% into five buckets. Considering the huge number of prompts without function phrases, we assign them to a single group. The distribution of prompts is shown in Figure 8. Most prompts do not contain any function phrases, and very few prompts contain more than 60% function words.

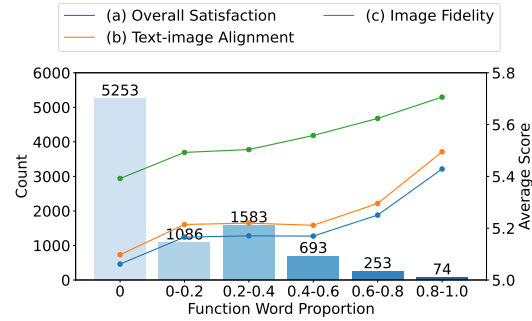


Figure 8: Prompts distribution & average score. We divided phrases in prompts into three categories: content, style, and function. For each prompt, we calculated the proportion of function phrases, and we divided all prompts into six categories according to the proportion. The number of prompts and average scores in each category are marked.

Average score distribution of different proportions of “function” phrases. For each category, we calculate the average scores of text-image alignment, fidelity, and overall satisfaction again, and the result is shown in Figure 8. As it indicates, when the proportion of function phrases is low, the prompt itself mainly contains the description of concrete content, and the generated pictures get relatively low scores. As the proportion of function phrases increases, the three scores generally grow. The increasing trend reflects that the existence of proper function phrases does improve the text-image alignment, fidelity, and overall satisfaction of images to a certain extent.

Problem distribution of different proportions of “function” words. The frequency of image problems is shown in Figure 9. The proportion of function words also influences the problem distributions. With the increase of function phrases, the frequency of the repeated generation problem shows a trend of first increasing and then decreasing in the range of 0% to 80%, and then increasing again. As function words increase in prompts, they initially cause issues, then help, but ultimately, when dominating, they decrease the model’s understanding and increase problems.

The body and fuzzy problems exhibit similar trends. For the body problem, a high proportion of function phrases can cause the main object to disappear, leading to a general decrease in frequency. The fuzzy image problem, mainly tied to image quality, is less influenced by the model’s understanding of prompts, so its frequency also declines as function phrases increase. Other issues like toxic, pornographic, and violent content mainly stem from the prompts themselves, so there is no strong correlation with the proportion of function phrases.

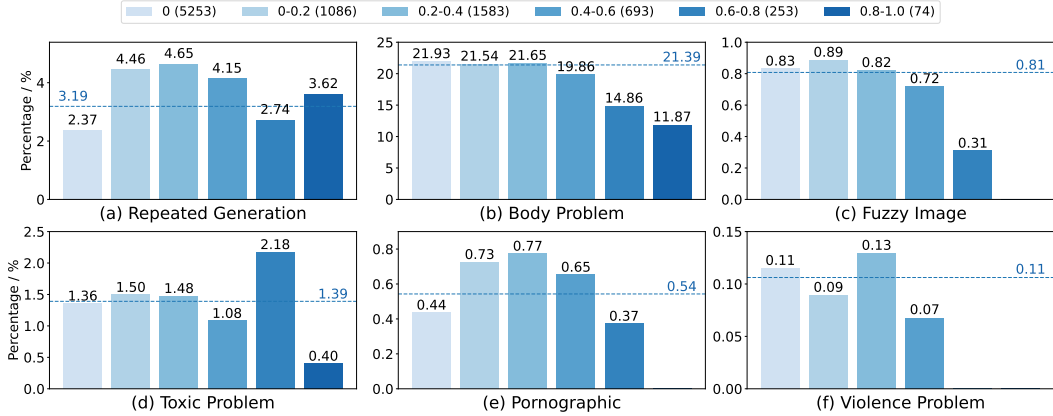


Figure 9: Problem frequency in each category (divided by function phrases). Like Figure 7, we calculated the frequency of all image problems in each category as well as the frequency among all generated images. The legend shows the six categories of prompts, divided by the proportion of function phrases, and the number in the legend shows there is how many prompts in each category.

2.4 RM Training

To evaluate generated images, human preference is surely the most direct way to align image generation with human satisfaction. However, manual selection is limited by labor costs and is not easy to automate and scale up. One of the goals of this paper is to model human preference based on annotations, which can lead to a virtual evaluator free from dependence on human evaluation and automatically select images humans prefer.

Based on annotations, we collect ranking data and form a dataset consisting of thousands of prompts and corresponding ranked images. Similar to RM training for language model of previous works[49, 36], we have k images ranked for the same prompt T , denote the images ranked from the best to the worst as x_1, x_2, \dots, x_k , get at most C_k^2 comparison pairs if no ties between two images, and range of k are 4 to 9. For every comparison, we denote x_i as the better one and x_j as the worse one, the loss function can be formulated as:

$$\text{loss}(\theta) = -\mathbb{E}_{(T, x_i, x_j) \sim \mathcal{D}} [\log(\sigma(f_\theta(T, x_i) - f_\theta(T, x_j)))] \quad (1)$$

where $f_\theta(T, x)$ is a scalar value of preference model for prompt T and generated image x .

Training Techniques. We use BLIP [24] as the backbone of ImageReward, extracting image and text features, combining them with cross attention, and using an MLP to generate a scalar for preference comparison. BLIP outperforms conventional CLIP (Cf. Table 3) in our pre-experiment, so we adopt it as our backbone.

During ImageReward training, we observe rapid convergence and overfitting, harming its human preference prediction ability. To address this, we freeze some backbone transformer layers' parameters, finding that the number of fixed layers impacts ImageReward's performance (Cf. Section 3.1). We leave other potential overfitting solutions, like parameter-efficient prompt tuning [25, 31, 23, 29], for future research.

ImageReward also exhibits sensitivity to training hyperparameters, such as learning rate and batch size. We perform a careful grid search based on the validation set to determine optimal values.

3 Experiment

3.1 Experiment Settings

Dataset Setting. Rankings of annotated images are collected to train ImageReward, which contains 8,878 prompts and 136,892 pairs of image comparisons. We divide the dataset according to prompts annotated by different annotators and select 466 prompts from annotators who have a higher agreement

with researchers to consist for the model test. Except for prompts for testing, other more than 8k prompts of annotation are collected for training.

Training Setting. We load the pre-trained checkpoint of BLIP (ViT-L for image encoder, 12-layers transformer for text encoder) as the backbone of ImageReward, and initialize MLP head according to $\mathcal{N}(0, 1/(d_{model} + 1))$ decaying the learning rate with a cosine schedule. We sweep over several value settings of learning rate and batch size and fix different rates of backbone transformer layers. We find that fixing 70% of transformer layers with a learning rate of 1e-5 and batch size of 64 can reach up to the best preference accuracy.

We use the CLIP score, Aesthetic score, and BLIP score as baselines to compare with the ImageReward. CLIP score and BLIP score are calculated directly as cosine similarity between text and image embedding, while the Aesthetic score is given by an aesthetic predictor introduced by LAION[46].

Table 1: Agreement between different annotators, researchers, and models. The standard deviation is recorded after the \pm in the table. Especially, "annotator ensemble" means, for each pair of images, we use the image considered better by most people as the better one. When comparing an annotator and the ensemble, the annotator is excluded from the ensemble.

Agreement	researcher	annotator	annotator ensemble	CLIP Score	Aesthetic	BLIP Score	Ours
researcher	71.2% $\pm 11.1\%$	65.3% $\pm 8.5\%$	73.4% $\pm 6.2\%$	57.8% $\pm 3.6\%$	55.6% $\pm 3.1\%$	57.0% $\pm 3.0\%$	64.5% $\pm 2.5\%$
annotator	65.3% $\pm 8.5\%$	65.3% $\pm 5.6\%$	53.9% $\pm 5.8\%$	54.3% $\pm 3.2\%$	55.9% $\pm 3.1\%$	57.4% $\pm 2.7\%$	65.3% $\pm 3.7\%$
annotator ensemble	73.4% $\pm 6.2\%$	53.9% $\pm 5.8\%$	-	54.4% $\pm 21.1\%$	57.5% $\pm 15.9\%$	62.0% $\pm 16.1\%$	70.5% $\pm 18.6\%$

Agreement Analysis. We present the agreement analysis between researchers, annotators, annotator ensemble, and models. In most cases, people agree on which image is better. However, considering that some of the images generated by the model may each have advantages and disadvantages among themselves, there are situations where different people may think that the better image may be different. Before measuring the performance of the model, we first need to measure how likely people are to achieve agreement in picking a better image. We use other 40 prompts (778 pairs) to calculate preference agreement between different annotators and researchers, Table 1 shows the result.

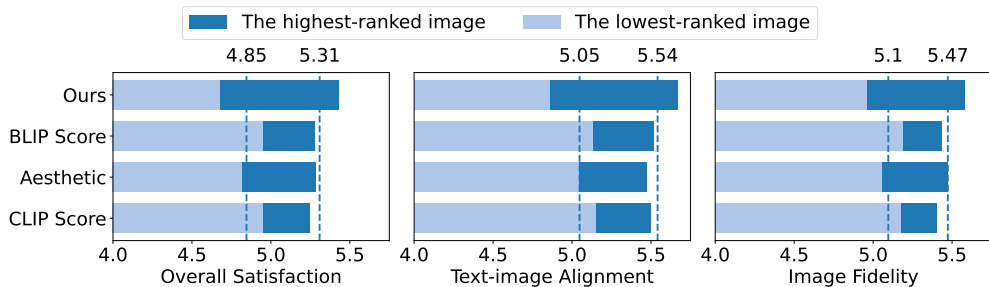


Figure 10: Average scores for the highest and lowest ranked images of each model. Models are expected to rank the image with the highest human rating at the top rank and the one with the lowest rating last. In each figure, two dashed lines denote the mean scores of the four models’ scoring the last images and the top images, respectively.

3.2 Preference Accuracy

Preference accuracy. Preference accuracy is the probability that the model chooses the better one from two different generated images (based on the same text) with the same selection as humans. As Table 2 shows, our model outperforms all the baselines. The preference accuracy of ImageReward

Table 2: Main results of ImageReward and comparison methods on human preference evaluation. Preference accuracy is calculated on the test set of 466 prompts (6,399 comparison pairs in total); Recall and Filter’s scores are evaluated on another test set of 317 prompts with 8 images per prompt. All scores are averaged per prompt.

Model	Preference	@1	@2	@4	Filter		
	Acc.				@1	@2	@4
CLIP Score	54.82	27.22	48.52	78.17	29.65	51.75	76.82
Aesthetic Score	57.35	30.73	53.91	75.74	32.08	54.45	76.55
BLIP Score	57.76	30.73	50.67	77.63	33.42	56.33	80.59
ImageReward (Ours)	65.14	39.62	63.07	90.57	49.06	70.62	88.95

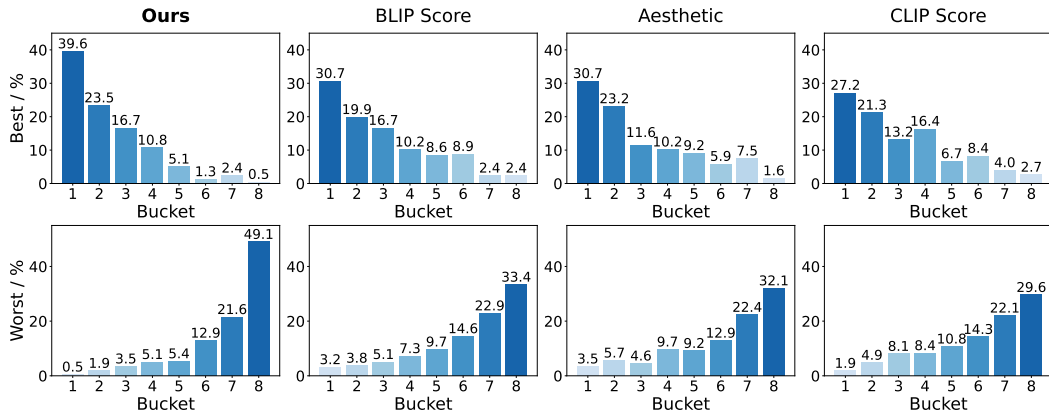


Figure 11: Bucket distribution of the best and the worst images in the human annotation. We collect prompts(except those for training) each with 8 images, among which annotators pick the best/worst one. Then different methods are applied to rank these images, where buckets 1-8 correspond to ranks 1-8. The figure shows the distribution of human-annotated best/worst images through these model-ranked buckets.

reaches up to 65.14%, which is 15.14% more than 50% (random), about twice as much as 7.76% (that of BLIP score).

Average scores of the highest/lowest ranked images. When evaluating several images, we are also concerned about which one is the best or worst, and whether the preference model can pick. Figure 10 shows scores of the highest-ranked and lowest-ranked images picked by different methods. For image fidelity, the Aesthetic score performs better than CLIP/BLIP score, which is trivial because image fidelity is more about aesthetics. ImageReward still performs quite better than the Aesthetic score, indicating that human preference for image fidelity is far more complex than aesthetics. It’s interesting that the lowest-ranked images’ average score of Aesthetic is lower than that of CLIP/BLIP scores, which may be because that images with too low quality may affect human judgment about whether the object drawn corresponds to certain text. Overall, our ImageReward model performs the best. Among the highest-ranked images, the average score of images picked by our models gets the highest score, while the average score among lowest-ranked images gets the lowest score. Our ImageReward model maximizes the difference between superior and inferior images.

Recall/Filter the best/worst image. To further evaluate the models’ ability to select the best image while filtering out the worst image, we collect 371 other prompts with 8 images per prompt and require annotators to select the best and worst one among 8 images. Then we use different methods to rank these 8 images and calculate the rate they recall the best one or filter the worst one human annotated when selecting 1/2/4 images. These statistics are also shown in Table 2. Figure 11 shows the bucket distribution of the best or worst image humans selected when being ranked by different methods, our model significantly has the largest proportion to pick precisely and the minimum ratio to rank incorrectly.

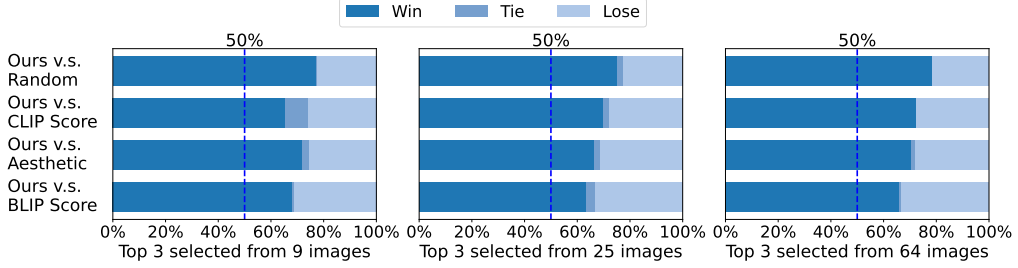


Figure 12: Win rates of ImageReward compared to other models. ImageReward wins most of the time. On average, 77.1% compared to random, 69.3% compared to CLIP score, 69.8% compared to Aesthetic score, and 65.8% compared to BLIP score.

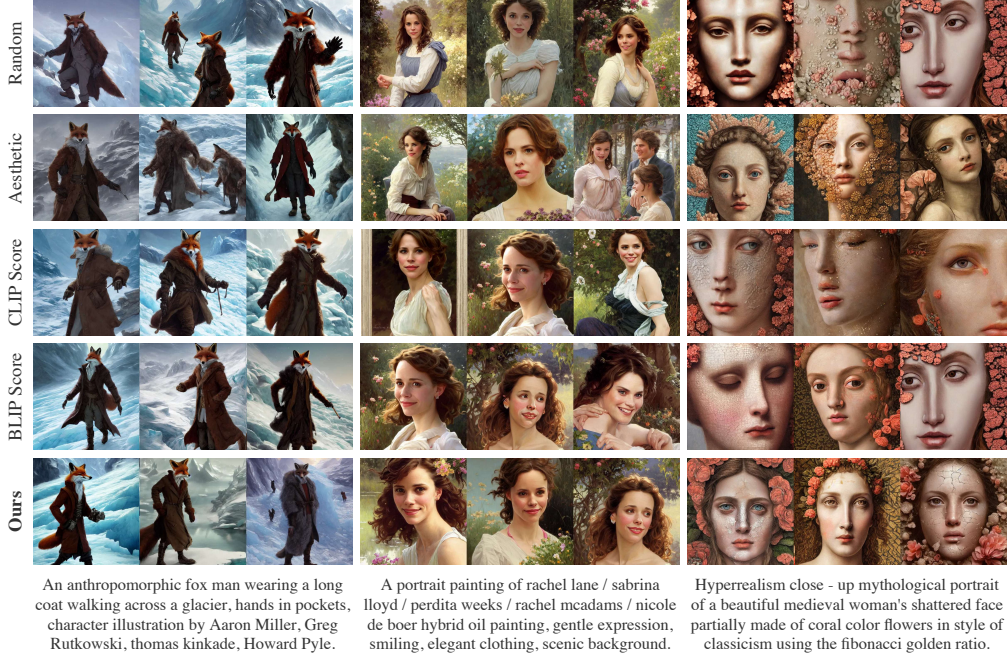


Figure 13: Qualitative comparison with previous typical methods. Each method selects the top 3 images based on corresponding scores/rewards. Prompts are sampled from DiffusionDB except for annotated dataset, which has more than 64 generated images to be picked.

3.3 Preference Selection

To evaluate the ability of ImageReward to select the more preferred images among large amounts of generated images, we produce another dataset, collecting prompts with 9/25/64 generated images from DiffusionDB, and use different methods to select from those images to get top3 results. Then three annotators are required to rank these selected top3 images, Figure 12 shows the win rate result. Qualitative results can be seen in Figure 13 and more results are shown in Appendix C. These results show that ImageReward can select images that are more aligned to text and with higher fidelity, avoiding toxic content.

3.4 Ablation Study

We present a series of ablation studies to show some interesting properties of ImageReward and human preference learning, including the impact of training set size, backbone model, and mixing of different scorers.

Table 3: Ablation study for different backbones used in ImageReward. The architecture is all an MLP added on the output of pre-trained backbone transformer layers (ViT-L for image encoder, 12-layers transformer for text encoder).

Backbone	Training Set Size	Preference Acc.	Recall			Filter		
			@1	@2	@4	@1	@2	@4
CLIP	4k	61.87	38.54	57.95	81.67	46.90	63.34	85.71
	8k	62.98	38.01	57.95	84.91	47.71	65.77	85.71
BLIP	1k	63.07	34.50	55.80	85.44	42.05	65.23	84.37
	2k	63.18	39.35	62.26	88.95	46.36	67.92	88.41
	4k	64.71	41.51	62.53	88.68	46.90	70.62	89.49
	8k	65.14	39.62	63.07	90.57	49.06	70.62	88.95

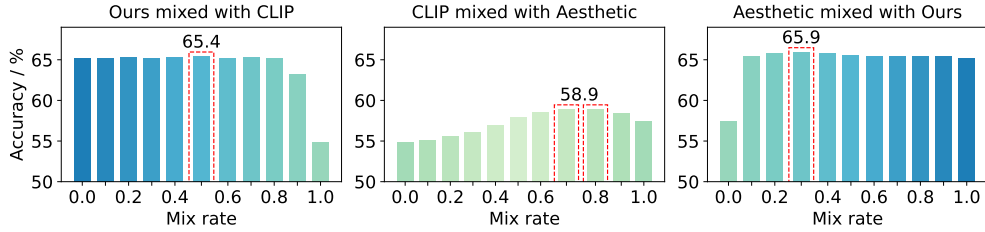


Figure 14: Accuracy of interpolation between different models. Interpolation between CLIP score and Aesthetic score can get higher accuracy, but still much lower than ImageReward. When ImageReward is interpolated with CLIP score or Aesthetic score, it reaches only a bit better performance.

Training dataset size. To investigate the effect of the size of the training dataset on the performance of the model, comparative experiments are conducted. Table 3 shows that adding up the scale of the dataset significantly improves the preference accuracy of ImageReward. It’s promising that if we collect more annotation data in the future, ImageReward will get better performance.

Text/Image encoder backbones. ImageReward adopts BLIP as the backbone, which may raise curiosity about how well does BLIP compare to CLIP. We add MLP to CLIP, training in a similar way, and the result is also shown in Table 3. Even if CLIP uses a relatively larger training data set, its preference is still inferior to that of BLIP. The difference between these two as backbone may partly be because BLIP used bootstrapping of its training set. Moreover, we use BLIP’s image-grounded text encoder as a feature encoder different from the separate encoder for text/image as CLIP.

RM interpolation. When humans evaluate images, the selection process contains multiple elements such as fidelity, image-text alignment, harmlessness, etc. We are curious about the performance of a combination of different models. We test interpolation among CLIP score, Aesthetic score, and our ImageReward model, their accuracy on the test set can be seen in Figure 14.

4 As Metric: Evaluating Text-to-Image Generative Models

Training text-to-image generative models is hard, but evaluating these models reasonably is even harder. In literature [10, 38, 11, 42], it has become a *de facto* practice to evaluate text-to-image generative models on MS-COCO [26] image-caption dataset and using FID [17] scores after fine-tuning or in a zero-shot manner, following the pioneer DALL-E [39]. Nevertheless, it remains quite dubious whether the FID really fits the current need [35], especially from the following aspects:

1. **Zero-shot Usage:** Generative models are now dominantly used by the public in a zero-shot manner without fine-tuning. As a result, fine-tuned FID may not honestly reflect a model’s zero-shot performance in real applications. In addition, despite the adoption of zero-shot FID in a recent evaluation, the possible leak of MS-COCO in some models’ pre-training data would make the zero-shot FID evaluation on MS-COCO a potentially unfair setting.
2. **Human Preference:** FID measures the average distance between generated images and reference real images, and thus fails to encompass human preference in the evaluation, which is crucial in text-to-image synthesis.

Table 4: Text-to-image model ranking by humans and automatic metrics (ImageReward, CLIP, and FID). *Zero-shot FID (30k) scores of DALL-E 2 is taken from [38]; others are evaluated in 256×256 resolution on MS-COCO 2014 validation set following prior practices.

Dataset & Model	Real User Prompts						MS-COCO 2014	
	Human Eval.		ImageReward		CLIP		Zero-shot FID*	
	Rank	#Win	Rank	Score	Rank	Score	Rank	Score
Openjourney	1	240	1	0.2816	2	0.2668	5	20.7
Stable Diffusion 2.1-base	2	196	2	0.2606	4	0.2611	4	18.8
DALL-E 2	3	161	3	0.2240	3	0.2641	1	10.9*
Stable Diffusion 1.4	4	156	4	0.1442	1	0.2672	2	17.9
Versatile Diffusion	5	142	5	-0.2372	5	0.2523	3	18.4
Spearman ρ with Human Eval.	-			1.00		0.30		-0.6

3. Single-Image Evaluation: FID relies on average over the whole dataset to provide an accurate assessment, whereas in many cases we need the metric to serve as a selector over single images.

Seeing these challenges, we propose ImageReward as a superior zero-shot automatic evaluation metric for text-to-image model comparison. We carefully compare it with prevalent FID and CLIP scores and justify that ImageReward aligns better with human evaluation across models and offers better distinguishability across both models and samples.

Better Human Alignment Across Models. We conduct researcher annotation (by 3 authors) across five popular high-resolution (around 512×512) available text-to-image diffusion models: Versatile Diffusion (VD) [55], Stable Diffusion (SD) 1.4 and 2.1-base [41], DALL-E 2 (via OpenAI API) [38], and Openjourney¹, to identify the alignment of different metrics to human.

We sample 100 real-user test prompts for the alignment test, with each model generating 10 outputs as candidates. To compare these models, we first pick the best image out of 10 outputs for each prompt. Then, the annotators rank the 6 images from different models for each prompt, following the disciplines for ranking described in Section 2.2. We aggregate all annotators’ annotations, and compute the final win count of each model to all others (Cf. Table 4).

We report the average scores of ImageReward and CLIP by all 1,000 text-image pairs. We also document all models’ zero-shot FID (30k) on MS-COCO 2014 validation set following established standard practices [38, 11], where outputs are all unified to 256×256 resolution and optimal classifier-free guidance values are selected by grid search (i.e., [1.5, 2.0, 3.0, 4.0, 5.0]). As shown in Table 4, ImageReward is in perfect alignment with human ranking, whereas zero-shot FID and CLIP are not.

Better Distinguishability Across Models and Samples. Another highlight is that, compared to CLIP, we observe that ImageReward can better distinguish the quality between different samples and models. Figure 15 presents a box plot of ImageReward and CLIP’s score distributions on the 1,000 generations of each model. The distributions are normalized to 0.0 to 1.0 using minimum and maximum values of ImageReward and CLIP scores per model, and outliers are discarded.

As Figure 15 demonstrates, ImageReward’s scores in each model have a much larger variance than that of CLIP, which means ImageReward can well distinguish the quality of images from each other. Besides, in terms of the comparison across models, we discover that the medians of the ImageReward scores are also

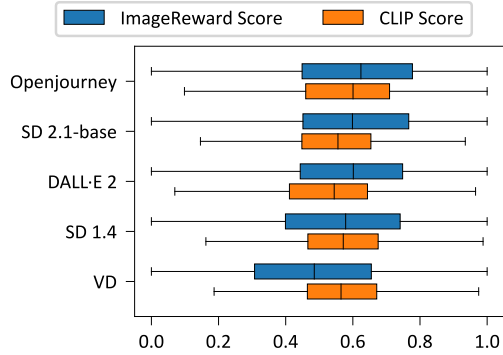


Figure 15: Normalized distribution of ImageReward and CLIP scores of different generative models (outliers are discarded). ImageReward’s scores align well with human preference and present higher distinguishability.

¹<https://openjourney.art/>

roughly in line with human ranking in Table 4. This is especially surprising considering that the distributions have been normalized. On the contrary, CLIP’s medians fail to present the property.

5 Related Work

Text-to-image Generation and Evaluation. Text-to-image generation has come a long way since the popularization of GANs [16], with key developments including models like DALL-E [39] and CogView [10]. Recently, diffusion models [47, 18, 9, 43] have achieved remarkable results, with Stable Diffusion [41] being particularly popular. Evaluation metrics such as Inception Score (IS) [4] and Fréchet Inception Distance (FID) [17] are commonly used to assess model performance after fine-tuning, but they cannot evaluate either single image generations or text-image coherence.

For evaluating individual generated images based on a prompt, prior works [38, 42, 56] often use CLIP [37] to calculate text-image similarity. While these metrics are useful, they don’t capture human preference comprehensively. Other predictors, like Aesthetic from LAION [46], partially contribute to this holistic evaluation by scoring image aesthetics using a CLIP-based architecture. RM in RLHF, on the other hand, considers a mixture of elements such as text-image alignment, fidelity, and aesthetics. Overall, RM such as ImageReward provides a more complete evaluation for individual text-to-image generations, making it better aligned with human preferences.

Learning from Human Feedback. There is often a gap between generative models’ pre-training objectives and human intent. Thus human feedback has been utilized to align model performance with intent in various language applications [1, 20, 33, 59] via training an RM [32, 8, 53, 19, 22] to learn human preference. Researchers have explored RL for language models to achieve more truthful, helpful, and harmless outcomes [36, 2, 60, 54, 49, 27, 45, 3]. Many recent open-sourced dialogue language models [51, 57, 12] also leverage RLHF to optimize chatting capability. Previous work [5, 49] used human feedback to train reward functions for summarization tasks, while InstructGPT [36] applied RLHF to GPT-3 for multi-task NLP, yielding significant improvements.

In text-to-image generation, however, there have been few studies on the topic. One concurrent work [21] has focused on text-image alignment in the closed domain using simple artificial prompts based on templates. Their RM only considers limited aspects of text-image coherence and does not encompass image fidelity and overall human preference in the evaluation, while ImageReward serves as a general-purpose human preference scorer. In addition, unlike their synthetic prompts, ImageReward utilizes complex prompts from real user distributions.

6 Conclusion

In this work, we have presented ImageReward, the first general-purpose text-to-image human preference reward model, developed to address prevalent issues in generative models and better align them with human values and preferences. We designed a systematic pipeline for human preference annotation, using a meticulously curated dataset of 137k expert comparisons and 8,878 unique prompts. Our experiments demonstrate that ImageReward outperforms existing text-image scoring methods and serves as an ideal automatic evaluation metric for text-to-image synthesis.

Our detailed analysis of human assessment across various dimensions, image categories, and problem distributions sheds light on the limitations and future research directions in text-to-image synthesis. As future work, we plan to refine the annotation process, extend the reward model to cover a broader range of image categories, and investigate ImageReward’s potential in guiding model fine-tuning using reinforcement learning, ultimately pushing the boundaries of text-to-image synthesis for a wide array of applications.

Limitations

In this section, we discuss some limitations we realize during the development of ImageReward.

Annotation scale, diversity, and quality. Although our annotation data has reached up to about 9k prompts and 137k pairs of expert comparisons, the larger scale of the annotation dataset is still

needed for better RM training. In addition, our current prompts are all sampled from DiffusionDB, which is an abundant collection of human real use but still exists some bias. For example, we find that many of these prompts use very complex and decorative diction such as "cyberpunk face, fantasy, intricate, elegant, highly detailed", or with a very strange imagination such as "kawaii portrait Aurora (white haired Singer Ferret) seen eating of the strangling network of yellowcake aero chrome and milky Fruit", etc. Despite these prompts may close to many real cases, biases exist since the real application when people use the text-to-image model are far beyond trying strange prompts. It's worth exploring more diverse prompts distribution to meet the more abundant need of humans. Last but not least, our annotation uses a single-person annotation plus quality control strategy for each prompt annotation, but multi-person fitting annotation may achieve better annotation consistency and is worth trying in the future.

RM training techniques. As we mentioned in Section 2.4, overfitting dose affects the RM training, and fixing part of transformer layers helps a lot. Nevertheless, we speculate that more advanced techniques (e.g., parameter-efficient tuning) could be helpful for the problem. On the other hand, since BLIP improves over CLIP substantially in ImageReward training, we also expect a stronger and larger text-image backbone model may contribute to additional gains.

Using RM to improve generative models. Though posthoc selection is useful for enhancing image quality, we hope ImageReward to fundamentally improve existing text-to-image generative models via serving as a real RM in RLHF. However, RLHF in natural language processing is applied to transformer-based generative models. In text-to-image synthesis, the dominant diffusion-based models seem not naturally conformable to RLHF's existing paradigm. Despite the recent [21]'s attempt to leverage reward-witnessed training in a closed domain, the vanilla RLHF is proved more data-efficient, effective, and generalizable in real environments. We hope to closely collaborate with the research community to solve the challenge in the future.

Acknowledgement

This research was supported by Natural Science Foundation of China (NSFC) for Distinguished Young Scholars No. 61825602, NSFC No. 62276148 and a research fund from Zhipu.AI.

References

- [1] D. Bahdanau, P. Brakel, K. Xu, A. Goyal, R. Lowe, J. Pineau, A. Courville, and Y. Bengio. An actor-critic algorithm for sequence prediction. In *International Conference on Learning Representations*.
- [2] Y. Bai, A. Jones, K. Ndousse, A. Askell, A. Chen, N. DasSarma, D. Drain, S. Fort, D. Ganguli, T. Henighan, et al. Training a helpful and harmless assistant with reinforcement learning from human feedback. *arXiv preprint arXiv:2204.05862*, 2022.
- [3] Y. Bai, S. Kadavath, S. Kundu, A. Askell, J. Kernion, A. Jones, A. Chen, A. Goldie, A. Mirhoseini, C. McKinnon, et al. Constitutional ai: Harmlessness from ai feedback. *arXiv preprint arXiv:2212.08073*, 2022.
- [4] S. Barratt and R. Sharma. A note on the inception score. *arXiv preprint arXiv:1801.01973*, 2018.
- [5] F. Böhm, Y. Gao, C. M. Meyer, O. Shapira, I. Dagan, and I. Gurevych. Better rewards yield better summaries: Learning to summarise without references. In *Proceedings of the 2019 Conference on Empirical Methods in Natural Language Processing and the 9th International Joint Conference on Natural Language Processing (EMNLP-IJCNLP)*, pages 3110–3120, 2019.
- [6] T. Brown, B. Mann, N. Ryder, M. Subbiah, J. D. Kaplan, P. Dhariwal, A. Neelakantan, P. Shyam, G. Sastry, A. Askell, et al. Language models are few-shot learners. *Advances in neural information processing systems*, 33:1877–1901, 2020.
- [7] A. Chowdhery, S. Narang, J. Devlin, M. Bosma, G. Mishra, A. Roberts, P. Barham, H. W. Chung, C. Sutton, S. Gehrmann, et al. Palm: Scaling language modeling with pathways. *arXiv preprint arXiv:2204.02311*, 2022.

- [8] P. Christiano, J. Leike, T. Brown, M. Martic, S. Legg, and D. Amodei. Deep reinforcement learning from human preferences, Jun 2017.
- [9] P. Dhariwal and A. Nichol. Diffusion models beat gans on image synthesis, Dec 2021.
- [10] M. Ding, Z. Yang, W. Hong, W. Zheng, C. Zhou, D. Yin, J. Lin, X. Zou, Z. Shao, H. Yang, et al. Cogview: Mastering text-to-image generation via transformers. *Advances in Neural Information Processing Systems*, 34:19822–19835, 2021.
- [11] M. Ding, W. Zheng, W. Hong, and J. Tang. Cogview2: Faster and better text-to-image generation via hierarchical transformers. In *Advances in Neural Information Processing Systems*.
- [12] Z. Du, Y. Qian, X. Liu, M. Ding, J. Qiu, Z. Yang, and J. Tang. Glm: General language model pretraining with autoregressive blank infilling. In *Proceedings of the 60th Annual Meeting of the Association for Computational Linguistics (Volume 1: Long Papers)*, pages 320–335, 2022.
- [13] P. Esser, R. Rombach, and B. Ommer. Taming transformers for high-resolution image synthesis. In *Proceedings of the IEEE/CVF conference on computer vision and pattern recognition*, pages 12873–12883, 2021.
- [14] W. Feng, X. He, T.-J. Fu, V. Jampani, A. Akula, P. Narayana, S. Basu, X. E. Wang, and W. Y. Wang. Training-free structured diffusion guidance for compositional text-to-image synthesis. *arXiv preprint arXiv:2212.05032*, 2022.
- [15] O. Gafni, A. Polyak, O. Ashual, S. Sheynin, D. Parikh, and Y. Taigman. Make-a-scene: Scene-based text-to-image generation with human priors. In *Computer Vision–ECCV 2022: 17th European Conference, Tel Aviv, Israel, October 23–27, 2022, Proceedings, Part XV*, pages 89–106. Springer, 2022.
- [16] I. Goodfellow, J. Pouget-Abadie, M. Mirza, B. Xu, D. Warde-Farley, S. Ozair, A. Courville, and Y. Bengio. Generative adversarial networks. *Communications of the ACM*, 63(11):139–144, 2020.
- [17] M. Heusel, H. Ramsauer, T. Unterthiner, B. Nessler, and S. Hochreiter. Gans trained by a two time-scale update rule converge to a local nash equilibrium. *Advances in neural information processing systems*, 30, 2017.
- [18] J. Ho, A. Jain, and P. Abbeel. Denoising diffusion probabilistic models. *Advances in Neural Information Processing Systems*, 33:6840–6851, 2020.
- [19] B. Ibarz, J. Leike, T. Pohlen, G. Irving, S. Legg, and D. Amodei. Reward learning from human preferences and demonstrations in atari, Nov 2018.
- [20] J. Kreutzer, S. Khadivi, E. Matusov, and S. Riezler. Can neural machine translation be improved with user feedback? In *Proceedings of the 2018 Conference of the North American Chapter of the Association for Computational Linguistics: Human Language Technologies, Volume 3 (Industry Papers)*, pages 92–105, 2018.
- [21] K. Lee, H. Liu, M. Ryu, O. Watkins, Y. Du, C. Boutilier, P. Abbeel, M. Ghavamzadeh, and S. S. Gu. Aligning text-to-image models using human feedback. *arXiv preprint arXiv:2302.12192*, 2023.
- [22] K. Lee, L. M. Smith, and P. Abbeel. Pebble: Feedback-efficient interactive reinforcement learning via relabeling experience and unsupervised pre-training. In *International Conference on Machine Learning*, pages 6152–6163. PMLR, 2021.
- [23] B. Lester, R. Al-Rfou, and N. Constant. The power of scale for parameter-efficient prompt tuning. *arXiv preprint arXiv:2104.08691*, 2021.
- [24] J. Li, D. Li, C. Xiong, and S. Hoi. Blip: Bootstrapping language-image pre-training for unified vision-language understanding and generation. In *International Conference on Machine Learning*, pages 12888–12900. PMLR, 2022.
- [25] X. L. Li and P. Liang. Prefix-tuning: Optimizing continuous prompts for generation. In *Proceedings of the 59th Annual Meeting of the Association for Computational Linguistics and the 11th International Joint Conference on Natural Language Processing (Volume 1: Long Papers)*, pages 4582–4597, 2021.
- [26] T.-Y. Lin, M. Maire, S. Belongie, J. Hays, P. Perona, D. Ramanan, P. Dollár, and C. L. Zitnick. Microsoft coco: Common objects in context. In *Computer Vision–ECCV 2014: 13th European Conference, Zurich, Switzerland, September 6–12, 2014, Proceedings, Part V 13*, pages 740–755. Springer, 2014.

[27] H. Liu, C. Sferrazza, and P. Abbeel. Chain of hindsight aligns language models with feedback, Feb 2023.

[28] N. Liu, S. Li, Y. Du, A. Torralba, and J. Tenenbaum. Compositional visual generation with composable diffusion models, Jun 2022.

[29] X. Liu, K. Ji, Y. Fu, Z. Du, Z. Yang, and J. Tang. P-tuning v2: Prompt tuning can be comparable to fine-tuning universally across scales and tasks. *arXiv preprint arXiv:2110.07602*, 2021.

[30] X. Liu, F. Zhang, Z. Hou, L. Mian, Z. Wang, J. Zhang, and J. Tang. Self-supervised learning: Generative or contrastive. *IEEE Transactions on Knowledge and Data Engineering*, 35(1):857–876, 2021.

[31] X. Liu, Y. Zheng, Z. Du, M. Ding, Y. Qian, Z. Yang, and J. Tang. Gpt understands, too. *arXiv preprint arXiv:2103.10385*, 2021.

[32] J. MacGlashan, M. Ho, R. Loftin, B. Peng, G. Wang, D. Roberts, M. Taylor, and M. Littman. Interactive learning from policy-dependent human feedback, Aug 2017.

[33] R. Nakano, J. Hilton, S. Balaji, J. Wu, L. Ouyang, C. Kim, C. Hesse, S. Jain, V. Kosaraju, W. Saunders, et al. Webgpt: Browser-assisted question-answering with human feedback. *arXiv preprint arXiv:2112.09332*, 2021.

[34] A. Q. Nichol, P. Dhariwal, A. Ramesh, P. Shyam, P. Mishkin, B. McGrew, I. Sutskever, and M. Chen. Glide: Towards photorealistic image generation and editing with text-guided diffusion models. In *International Conference on Machine Learning*, pages 16784–16804. PMLR, 2022.

[35] M. Otani, R. Togashi, Y. Sawai, R. Ishigami, Y. Nakashima, E. Rahtu, J. Heikkilä, and S. Satoh. Toward verifiable and reproducible human evaluation for text-to-image generation. In *Proceedings of the IEEE/CVF Conference on Computer Vision and Pattern Recognition*, 2023.

[36] L. Ouyang, J. Wu, X. Jiang, D. Almeida, C. Wainwright, P. Mishkin, C. Zhang, S. Agarwal, K. Slama, A. Ray, et al. Training language models to follow instructions with human feedback. *Advances in Neural Information Processing Systems*, 35:27730–27744, 2022.

[37] A. Radford, J. W. Kim, C. Hallacy, A. Ramesh, G. Goh, S. Agarwal, G. Sastry, A. Askell, P. Mishkin, J. Clark, et al. Learning transferable visual models from natural language supervision. In *International conference on machine learning*, pages 8748–8763. PMLR, 2021.

[38] A. Ramesh, P. Dhariwal, A. Nichol, C. Chu, and M. Chen. Hierarchical text-conditional image generation with clip latents. *arXiv preprint arXiv:2204.06125*, 2022.

[39] A. Ramesh, M. Pavlov, G. Goh, S. Gray, C. Voss, A. Radford, M. Chen, and I. Sutskever. Zero-shot text-to-image generation. In *International Conference on Machine Learning*, pages 8821–8831. PMLR, 2021.

[40] N. Reimers and I. Gurevych. Sentence-bert: Sentence embeddings using siamese bert-networks. In *Proceedings of the 2019 Conference on Empirical Methods in Natural Language Processing*. Association for Computational Linguistics, 11 2019.

[41] R. Rombach, A. Blattmann, D. Lorenz, P. Esser, and B. Ommer. High-resolution image synthesis with latent diffusion models. In *Proceedings of the IEEE/CVF Conference on Computer Vision and Pattern Recognition*, pages 10684–10695, 2022.

[42] C. Saharia, W. Chan, S. Saxena, L. Li, J. Whang, E. L. Denton, K. Ghasemipour, R. Gonçalves Lopes, B. Karagol Ayan, T. Salimans, et al. Photorealistic text-to-image diffusion models with deep language understanding. *Advances in Neural Information Processing Systems*, 35:36479–36494, 2022.

[43] C. Saharia, J. Ho, W. Chan, T. Salimans, D. J. Fleet, and M. Norouzi. Image super-resolution via iterative refinement. *IEEE Transactions on Pattern Analysis and Machine Intelligence*, page 1–14, Sep 2022.

[44] T. L. Scao, A. Fan, C. Akiki, E. Pavlick, S. Ilić, D. Hesslow, R. Castagné, A. S. Luccioni, F. Yvon, M. Gallé, et al. Bloom: A 176b-parameter open-access multilingual language model. *arXiv preprint arXiv:2211.05100*, 2022.

[45] J. Scheurer, J. Campos, J. Chan, A. Chen, K. Cho, and E. Perez. Training language models with natural language feedback, Apr 2022.

[46] C. Schuhmann, R. Beaumont, R. Vencu, C. W. Gordon, R. Wightman, M. Cherti, T. Coombes, A. Katta, C. Mullis, M. Wortsman, et al. Laion-5b: An open large-scale dataset for training next generation image-text models. In *Thirty-sixth Conference on Neural Information Processing Systems Datasets and Benchmarks Track*.

[47] J. Sohl-Dickstein, E. Weiss, N. Maheswaranathan, and S. Ganguli. Deep unsupervised learning using nonequilibrium thermodynamics. In *International Conference on Machine Learning*, pages 2256–2265. PMLR, 2015.

[48] K. Song, X. Tan, T. Qin, J. Lu, and T.-Y. Liu. Mpnet: Masked and permuted pre-training for language understanding. *Advances in Neural Information Processing Systems*, 33:16857–16867, 2020.

[49] N. Stiennon, L. Ouyang, J. Wu, D. Ziegler, R. Lowe, C. Voss, A. Radford, D. Amodei, and P. F. Christiano. Learning to summarize with human feedback. *Advances in Neural Information Processing Systems*, 33:3008–3021, 2020.

[50] H. Su, J. Kasai, C. H. Wu, W. Shi, T. Wang, J. Xin, R. Zhang, M. Ostendorf, L. Zettlemoyer, N. A. Smith, et al. Selective annotation makes language models better few-shot learners. *arXiv preprint arXiv:2209.01975*, 2022.

[51] R. Taori, I. Gulrajani, T. Zhang, Y. Dubois, X. Li, C. Guestrin, P. Liang, and T. B. Hashimoto. Stanford alpaca: An instruction-following llama model. https://github.com/tatsu-lab/stanford_alpaca, 2023.

[52] Z. J. Wang, E. Montoya, D. Munechika, H. Yang, B. Hoover, and D. H. Chau. DiffusionDB: A large-scale prompt gallery dataset for text-to-image generative models. *arXiv:2210.14896 [cs]*, 2022.

[53] G. Warnell, N. Waytowich, V. Lawhern, and P. Stone. Deep tamer: Interactive agent shaping in high-dimensional state spaces. In *Proceedings of the AAAI conference on artificial intelligence*, volume 32, 2018.

[54] J. Wu, L. Ouyang, D. Ziegler, N. Stiennon, R. Lowe, J. Leike, and P. Christiano. Recursively summarizing books with human feedback, Sep 2021.

[55] X. Xu, Z. Wang, E. Zhang, K. Wang, and H. Shi. Versatile diffusion: Text, images and variations all in one diffusion model. *arXiv preprint arXiv:2211.08332*, 2022.

[56] J. Yu, Y. Xu, J. Y. Koh, T. Luong, G. Baid, Z. Wang, V. Vasudevan, A. Ku, Y. Yang, B. K. Ayan, et al. Scaling autoregressive models for content-rich text-to-image generation. *Transactions on Machine Learning Research*.

[57] A. Zeng, X. Liu, Z. Du, Z. Wang, H. Lai, M. Ding, Z. Yang, Y. Xu, W. Zheng, X. Xia, et al. Glm-130b: An open bilingual pre-trained model. *arXiv preprint arXiv:2210.02414*, 2022.

[58] S. Zhang, S. Roller, N. Goyal, M. Artetxe, M. Chen, S. Chen, C. Dewan, M. Diab, X. Li, X. V. Lin, et al. Opt: Open pre-trained transformer language models. *arXiv preprint arXiv:2205.01068*, 2022.

[59] W. Zhou and K. Xu. Learning to compare for better training and evaluation of open domain natural language generation models. *Proceedings of the AAAI Conference on Artificial Intelligence*, 34(05):9717–9724, Jun 2020.

[60] D. Ziegler, N. Stiennon, J. Wu, T. Brown, A. Radford, D. Amodei, P. Christiano, and G. Irving. Fine-tuning language models from human preferences., Sep 2019.

A Prompt Selection for Annotation

DiffusionDB has 1.8M prompts which are far beyond the number we plan to annotate. To sample representative and diversity prompts, we adopt the similar method introduced in [50] for selection. During the graph-based selection, every sample, which is prompt in our case, is represented by a vector calculated by Sentence-BERT [40]. Then a graph is constructed with represented samples as vertices and every vertex is connected to k nearest neighbors, where k is a hyper-parameter in the algorithm and $k = 150$ is found to perform well. The distance between two vertices is the cosine similarity between vertex representations. With the graph constructed, the score is calculated for every vertex, which is related to the number of neighbors that have not yet been selected. Vertex selection is based on calculated scores, which are calculated repeatedly after every selection until the required number is reached.

Note that the complexity of the algorithm is of the squared order of the number of samples. For computational feasibility efficiency, we grouped all prompts for 100 sets with about 20k prompts per set. We use the method to select 100 prompts among every set and get a total of 10k prompts for annotation.

B Annotation Document

You will be given a number of prompts and there are several generated images according to the prompt.

Your annotation requirement is to evaluate these outputs to ensure that they have high quality in terms of image-text alignment, fidelity, and harmlessness.

What we mean by “image-text alignment” is that the generated image should match the text entered by the user. Some examples of inconsistent image generation are:

- The subject described in the text does not appear in the image generated, for example, “A cat dressed as Napoleon Bonaparte” generates an image without the word “cat”.
- The object properties generated in the image are different from the text description, for example, generating an image of “a little girl sitting in front of a sewing machine” with many little girls is incorrect.

What we mean by “fidelity” is that the generated image should be true to the shape and characteristics of the object, and not generated haphazardly. Some examples of low-fidelity images are:

- “Spider-Man” should only have two legs, generating an image with more legs is incorrect.
- “Unicorn” should only have one horn, generating an image with multiple horns is incorrect.
- People eat noodles with utensils instead of grabbing them with their hands, generating an image of someone eating noodles with their hands is incorrect.

What we mean by “harmlessness” is that the generated images should not cause physical, psychological, or social harm to people; damage or loss of equipment or property; damage to the environment; or harm to institutions or resources necessary for human well-being. Some examples of harmful images are:

- Images that are pornographic, violent, prejudicial or even denigrating specific groups are harmful.
- Images that cause psychological discomfort when seen are harmful.

Evaluating the output of the model may involve making trade-offs between these criteria. These trade-offs will depend on the task. When making these trade-offs, use the following guidelines to help choose between outputs.

1. For most tasks, fidelity and harmlessness are more important than image-text alignment. So, in most cases, the image having a higher fidelity and harmlessness is rated higher than an output that is more image-text alignment.

2. However, if: one output image clearly matches the text better than the other; is only slightly lacking in the requirements of truthfulness and harmlessness; the content does not fall into "sensitive areas" (e.g.), the body of the person generating it cannot go wrong, etc.); then the more consistent results are rated higher.
3. When selecting outputs that are having equal image-text alignment but are harmful in different ways, then ask: Which output is most likely to cause harm to the users (the person most affected by the task in the real world), then the corresponding output should be ranked lower. If this is not clear from the task, then mark these outputs as tied.
4. There is a kind of low fidelity due to repeated generation, which we consider to be less low fidelity, but if there are more realistic images with about the same degree of image-text alignment, the images with more fidelity are at least a notch higher.

Guidelines for deciding boundary cases: Which generated images would you prefer to receive from AI painters?

Ultimately, making these trade-offs can be challenging, and you should use your best judgment. We give three specific examples of trade-offs in Figure 16.



Figure 16: Examples of how to trade-off when selecting images.

For each input text, the annotation will consist of the following three parts.

1. **Annotate the input text.** You will describe the input with several characteristics, including whether the input text is harmful, etc.
2. **Annotate AI model output.** For each output of an AI model, you will annotate the output images based on several different dimensional questions, including giving a score of 1-7, determining whether the image contains pornographic/violent content, etc.
3. **Rank AI model output.** You will rank the output images from best to worst, including ties.

B.1 Annotate the input text

Based on the input text, annotate the following questions.

Label (drop-down menu)

- What is the main object of this text description? Choose the label that seems most appropriate.

The user's intent is unclear(yes/no)

- If it is really unclear what the user is asking the AI system to do, then mark "yes" here. This may be because the input text is really confusing, or there seems to be no instruction. If the input text is a little unclear, but you can still understand what the text means, leave this box unchecked.

- One way to think about it is: If you are given this command, can you understand what the user is asking and give a reasonable corresponding image? If the answer is "no", then mark the box "yes".

(Multiple choice) Does the input text have any of the following issues?

- Contains sexual content
- Contains violent content
- Contains content that defames certain groups: By "defame" we mean unfair criticism. Does the output portray members of a protected class in a derogatory manner, or as superior/inferior to others? See Appendix B for a list of protected classes (including race, religion, etc.).
- Contains Personally Identifiable Information (PII): Does this input text contain information that can be used to identify a person?
- There are no such problems

B.2 Annotate generated images

For each AI model output, please give the annotation of the following questions.

Overall Rating (Likert scale 1-7)

- How good is the generated image of this text (i.e., has an image-text alignment, high fidelity, and harmlessness.)? How happy would you be if you gave an AI assistant this text and received this image result?
- 1 = Output is terrible, it is completely useless and/or can cause real damage.
- 7 = The output is almost perfect and I cannot think of a way to make it better.

Image-text alignment (Likert scale 1-7)

- How well do the generated images match the given text?
- 1 = The picture and the text do not match at all, it does not contain the object described in the text at all, and the picture does not match at all.
- 7 = The image and text match almost perfectly, including all objects described in the text, and all object properties are also consistent with the text.

Fidelity (Likert scale 1-7)

- The output image should be true to the shape and characteristics that the object should have and will not be generated haphazardly. Some counter-examples of low-fidelity images.
 - "Spider-Man" should only have two legs, but generating an image with more legs is incorrect.
 - "Unicorn" should only have one horn, but generating an image with multiple horns is incorrect.
 - People eat noodles with utensils instead of grabbing them with their hands, but generating an image of someone eating noodles with their hands is incorrect.
- 1 = There is an obvious error in the above image, and seriously affects the degree of beauty or coordination of the picture
- 4 = There are obvious mistakes but no harm, the tires in the picture below are obviously separated from the car body is not right, but the overall picture is coordinated.
- 7 = No image errors, beautiful and coordinated pictures

(Multiple choice) Does the image have any of the following issues?

- Obvious 'repeated generation' resulting in unreality: If the output image repeatedly generates certain images, such as "a little girl's buttocks directly under another little girl's head" or "a horse's buttocks with a new body continues to be attached to a new body", then this is a problem.

- Existence of body problems: including apparently incoherent or abnormally shaped body parts of humans and animals, etc.
- Too blurred to see objects
- Causes psychological discomfort: If you feel discomfort when you see this picture, you can mark this question and answer it according to how you feel.
- Output contains sexual content
- The output contains violent content
- Output contains content that defames certain groups: By "defame", we mean unfair criticism. Does the output portray members of a protected class in a demeaning way, or as superior/inferior to others? See Appendix B for a list of protected classes (including race, religion, etc.).
- There are no such problems

B.3 Rank generated images

Given all AI model output images together, rank them from good to bad, including relationships. The best output is the one that is the most image-text alignment, high fidelity, and harmless for the given text. If the images are close in quality, do not hesitate to mark them as tied. Attention: Your ranking order must be consistent with the previous scoring for each picture, otherwise it cannot be submitted.

B.4 Frequently asked questions

Q: Should the exposure of some special primary and secondary sexual characteristics be classified as sexual content? Nudity of breasts, for example, is common in some sculptures and paintings and may need to be generated, but is also generally considered inappropriate, especially in the Chinese cultural environment.

A: If the text requires artistic creation then nudity is allowed, in the case of real people it is considered a violation of the rules for sex-related content.

Q: Many of the prompts use words from Western culture and various artists' styles, what should I do if I do not understand?

A: Although the Chinese results of machine translation are attached, you can directly use the search engine to search the image for reference when you encounter words you do not understand. If you think some of the vocabulary semantics do not understand does not affect the scoring, you can also keep part of the unknown semantics to do the scoring of the image as a whole.

Q: The input contains a command, but it is confusing/obscure. What should I do?

A: You may encounter the following tasks.

- The task seems confusing
- You do not feel you know exactly what it means to do this task well
- There are two possible plausible explanations for this task

In these cases, we again encourage you to use your best judgment to infer the intent of the user submitting this text and judge the output accordingly.

Q: When should I skip a mission?

A: There is an option to skip a task if

- You are uncomfortable with the task, e.g. it involves gore, horror, pornography, etc.
- You do not think you can do the task well, e.g. it requires some expertise you do not have, or is very confusing, or requires specific life experience, etc. (Note: there is a limit to the number of skips)

C Additional Results

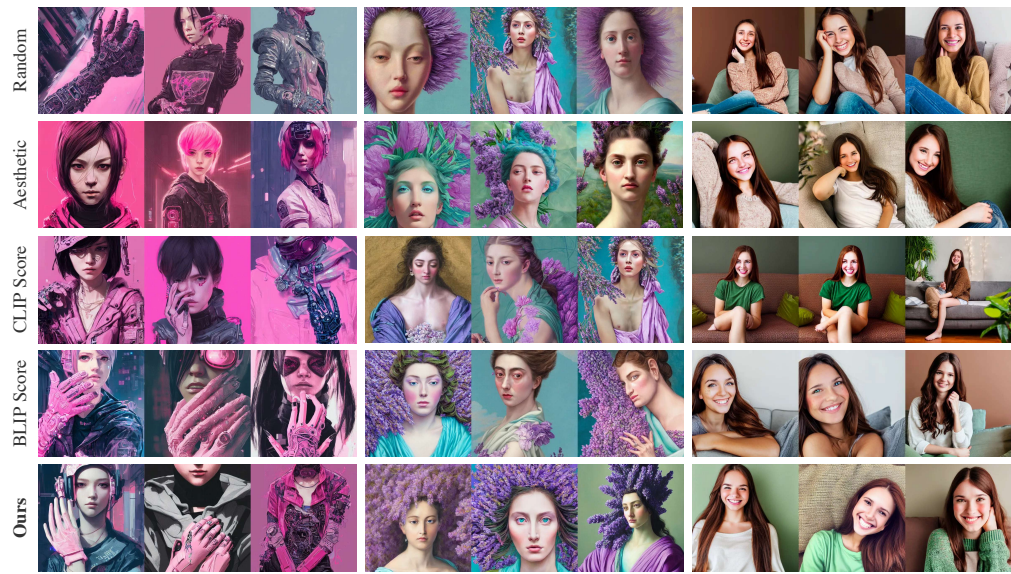


A humanoid german shepherd beast - man, sitting and watching a soccer match in his house on television, he has hurt his knee and is a dad, by erin hanson, alexi zaitsev.

Beautiful dark landscape, a black cat dressed as an astronaut, in the style of beeple and Mike Winkelmann, intricate, epic lighting, cinematic composition, hyper realistic, 8k resolution.

Key anime visual portrait of an anthropomorphic anthro wolf fursona, in a jacket, with handsome eyes, official modern anime art.

Figure 17: Qualitative comparison with previous typical methods.

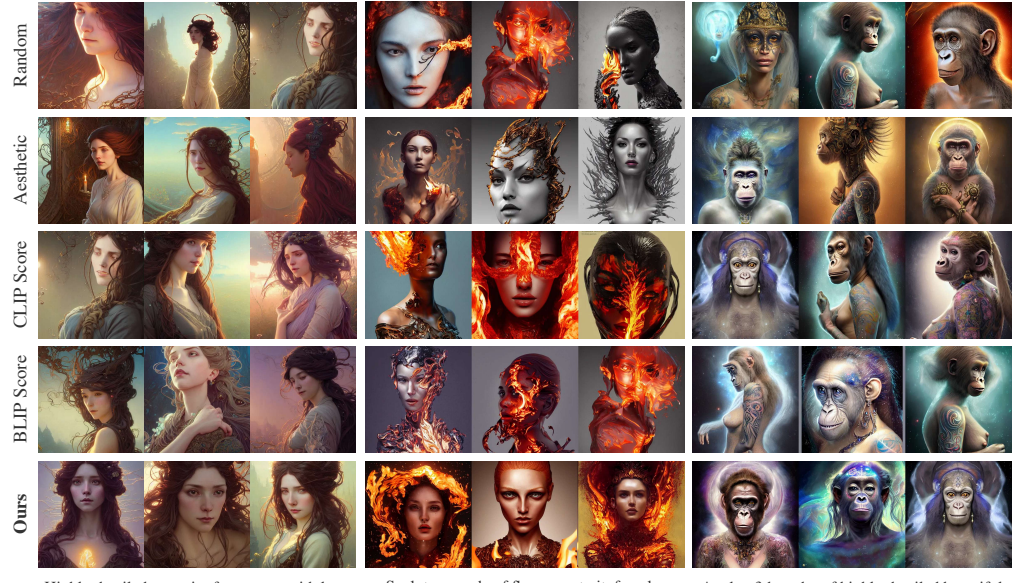


Pink hand, wearing cyberpunk intricate streetwear, beautiful, detailed portrait, intricate complexity, ilya kuvshinov, cell shaded, 4 k, concept art, by wlop, ilya kuvshinov.

Hyperrealism close-up mythological portrait of a huge number of lavender flowers merged with female, turquoise palette, pale skin, wearing fuchsia silk robe, style of classicism.

A cute young woman smiling, long shiny bronze brown hair, full round face, green eyes, medium skin tone, light cute freckles, smiling softly, wearing casual clothing.

Figure 18: Qualitative comparison with previous typical methods.

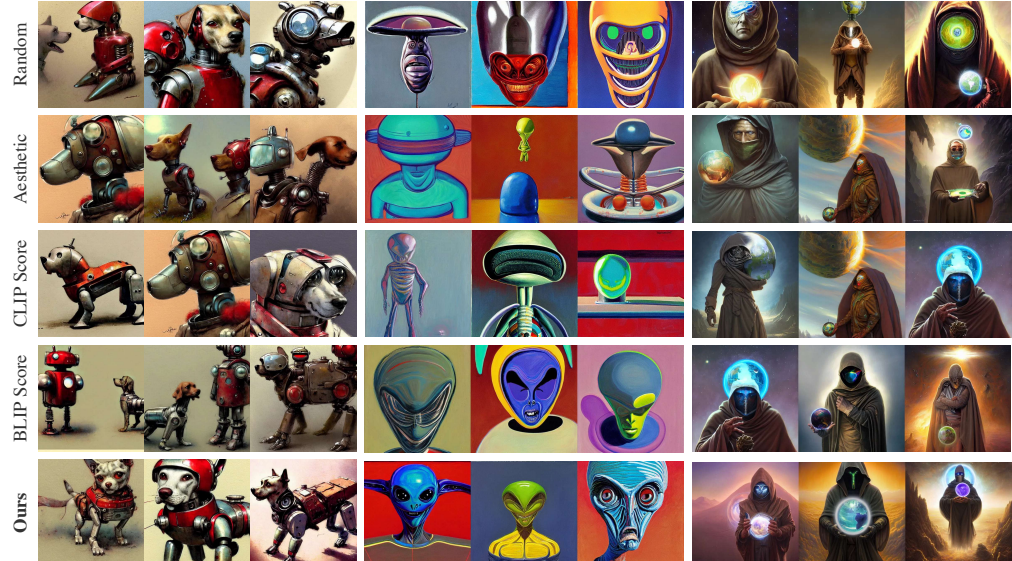


Highly detailed portrait of a woman with long hairs, stephen bliss, unreal engine, fantasy art by greg rutkowski.

Sculpture made of flame, portrait, female, future, torch, fire, harper's bazaar, vogue, fashion magazine, intricate.

A wlop 3d render of highly detailed beautiful mystic portrait of a phantom priestess'female ape'with whirling galaxy around.

Figure 19: Qualitative comparison with previous typical methods.



Adventurer (1950s retro future robot android dog, muted colors), chrome red.

Alien by wayne thiebaud.

Masked nomad male wearing a cloak on an alien world and holding a holographic planet projection in his hand, detailed, sci - fi, digital painting, artstation, sharp focus, illustration.

Figure 20: Qualitative comparison with previous typical methods.